Statistical Analyses of the Magnet Data for the Advanced Photon Source Storage Ring Magnets*

S. H. Kim, D. W. Carnegie, C. Doose, R. Hogrefe, K. Kim and R. Merl
Argonne National Laboratory, Argonne, IL 60439 USA

Abstract

The statistics of the measured magnetic data of 80 dipole, 400 quadrupole, and 280 sextupole magnets of conventional resistive designs for the APS storage ring is summarized. In order to accommodate the vacuum chamber, the curved dipole has a C-type cross section and the quadrupole and sextupole cross sections have 180˚ and 120˚ symmetries, respectively. The data statistics include the integrated main fields, multipole coefficients, magnetic and mechanical axes, and roll angles of the main fields. The average and rms values of the measured magnet data meet the storage ring requirements.

I. INTRODUCTION

The Advanced Photon Source (APS), now undergoing commissioning for operations at Argonne National Laboratory, is a national facility dedicated to providing highly-brilliant synchrotron radiation beams [1]. The APS accelerator system consists of a 7-GeV positron storage ring (SR), an injector synchrotron, a positron accumulator ring, and a linear accelerator. The 1104-m-circumference SR has 40 sectors of Chasman-Green lattice with two dipole, ten quadrupole (quad), seven sextupole (sext), and eight corrector magnets in each sector. The main parameters for the SR magnets are listed in Table 1. The five quad families have three different magnetic lengths with the same two-dimensional (2-D) geometry and a bore radius of 40.0 mm. The four sext families are the same design with a bore radius of 49.0 mm. The 80 dipole magnets are excited by a single power supply and the 400 quads and 280 sexts by individual power supplies. The required beam stay-clear aperture is x = ± 35 mm and y = ± 25 mm.

The integrated fields and field qualities for all SR magnets have been measured and evaluated to a few parts in 10^{-4} to verify the tolerance requirements. The magnetic and mechanical axes and roll angles with repect to the fiducials located on top of the magnets were measured within tolerances of 0.060 mm and 0.3 mrad, respectively. This paper summarizes the statistics of the measured magnet data for the SR magnets.

II. DESCRIPTION OF THE MAGNETS

In spite of the conventional nature of the magnets, the designs of the magnet cross sections are severely constrained to accommodate the vacuum chamber with its antechamber. Because of this requirement, rotation symmetries of 180˚ and 120˚ have been chosen for the quad and sext magnets, respectively, to minimize the undesired multipole field components. The cores of the magnets use 1.52-mm-thick laminations of low-carbon steel, coated on both sides with "C5" or a 13-μm-thick "B-stage" epoxy.

The C-type lamination core of the dipole magnet is stacked with a bending radius of 38.9611 m. The end-packs for both ends of the lamination core are assembled with 20 laminations. The pole-end bevels are designed so that the integrated and 2-D field shapes within ± 25 mm in the transverse direction are not significantly different. Before magnetic measurements, the production dipoles were installed on girders and corrected for any mechanical distortions of the magnets along their lengths.

In order to accommodate the vacuum chamber, the top and bottom halves of the quad are not connected with flux-return yokes; they are connected mechanically with aluminum spacers between the halves [2]. Each of the top and bottom halves consists of two welded quadrant stacks. The magnet has pole-end bevels and pole chamfers.

Table 1
Main parameters for the SR magnets.
The quads have five families and the sexts have four.
Quad aperture radius=40.0 mm, Sext aperture radius=49.0 mm

Dipoles	B (T)	l (m)	Bρ (Tm)	I (A)	Pole Gap (mm)
80	0.5991	3.06	23.349	450	60.0

Quads	Q_1	Q_2	Q_3	Q_4	Q_5
# Magnet	80	80	80	80	80
l (m)	0.50	0.80	0.50	0.50	0.60
B' (T/m)	-10.84	15.79	-10.59	-18.90	18.25
I (A)	215	312	210	386	370

Sexts	S_1	S_2	S_D	S_F
# Magnet	80	80	80	40
l (m)	0.2527	0.2527	0.2527	0.2527
B" (T/m^2)	185.07	-359.59	-415.0	192.62
I (A)	64	135	160	67

The cores of the sext magnet are assembled from three identical stacks of laminations, each with two poles and a flux-return path joining them [2]. The vacuum chamber extends into one of the 102-mm air gaps between neighboring stacks. At each end, 12.7-mm-thick stainless steel plates hold the core sections in position; they are pinned and bolted to the core sections with an assembly fixture. The assembly of the magnet using the stainless steel plates is designed so that the upper two poles of the magnet core can be moved for installation of the vacuum chamber.

*Work supported by the U.S. Department of Energy, Office of Basic Energy Sciences, under Contract No. W-31-109-ENG-38.

III. MEASURED MAGNETIC DATA STATISTICS

A. Dipole Data

The production dipoles were measured comparatively with respect to a reference dipole. Two sets of curved coils were connected in series, one fixed in the reference and one in the testing production magnet. The integrated field strengths were measured by ramping the excitation current of the dipole up and down while the field shapes were measured by moving the coil set in a transverse direction. A second reference dipole was used to check the effects of the large number of pulses of the first reference dipole during the production measurements. The probe coils are flat printed circuit coils connected in series according to the curvature of the magnet. A printed circuit coil is 0.5 m long with an average width of 6.8 mm, height of 3.3 mm, and 170 turns [3].

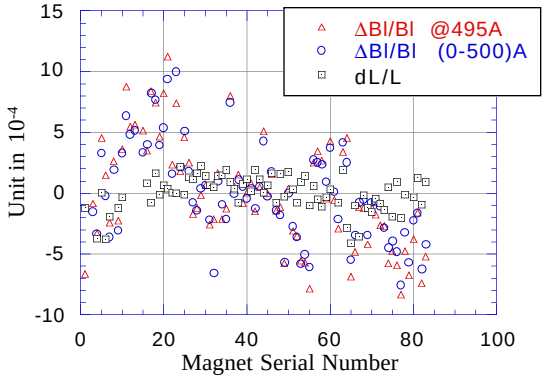

Fig. 1. Variations of the integrated fields and core lengths for the SR dipole magnets.

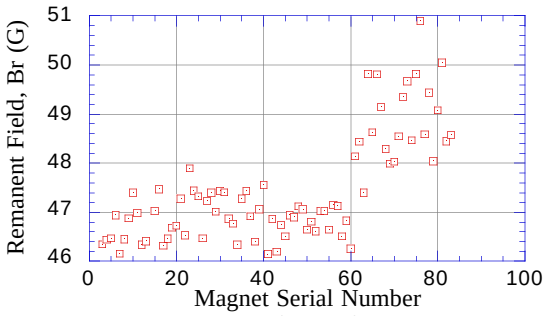

Fig. 2. Remanent fields of the SR dipoles.

Figures 1 and 2 show the relative variations of integrated fields at 495A, 0-500A, lamination core lengths, and remanent dipole fields for the dipole magnets. It is seen that, for magnets with serial numbers 61-83, the integrated fields are weaker by approximately 5 x 10^{-4} on average. At the same time, the remanent fields are higher by 2 Gauss. It is clear that these differences are due to different lamination properties. The root-mean-square (rms) values of the integrated fields are approximately 2.5 times that of the core lengths due to the tolerances of mechanical dimensions of the magnets. Because of these weaker dipoles with higher remanent fields, the histogram of the integrated fields for the dipoles in Fig. 3 is shifted toward the negative side. During compilation of the production magnet measurements, conducted for over a year, the measurement repeatability for the reference magnet was (2 ± 1.5) x 10^{-4}.

The variations of the integrated fields within ±25 mm of the transverse positions were less than 1.5 x 10^{-4} . The quad and sext coefficients obtained from a least square fit of the field variations in the midplane of the pole gap are shown in Fig. 4. Overall, the coefficients at the operating current of 450A are less than 1.5 x 10^{-4} .

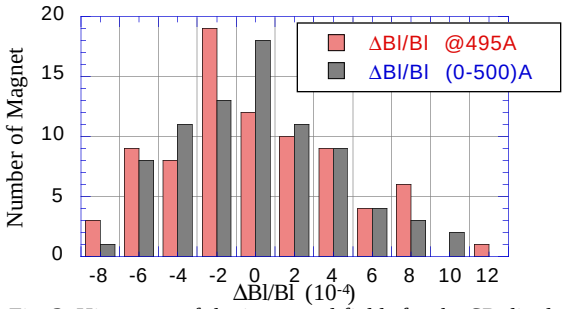

Fig. 3. Histogram of the integrated fields for the SR dipoles.

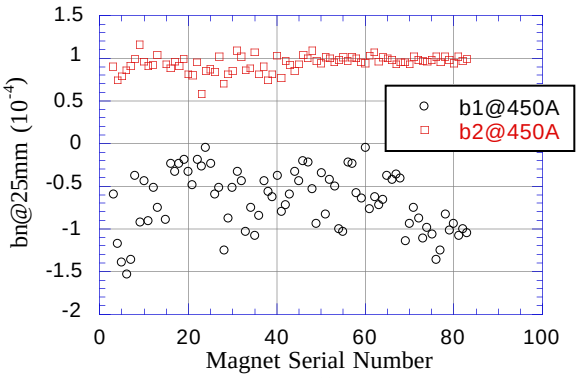

Fig. 4. Quad and sext coefficients within x=±25 mm in the midplane of the SR dipoles.

B. Quadrupole Magnet Data

The integrated fields and multipole field coefficients were measured using a rotating coil technique. The probe coil consists of "radial" and "tangential" coils on one cylinder [3]. The integrated field quality of a 2-D magnetic field in Cartesian coordinates, $B = B_y + i\,B_x$, is expressed in terms of dimensionless normal and skew multipole field coefficients, b_n and a_n,

$$Bl = B_o\, l \sum_{n=0}^{\infty} (b_n + i\, a_n)\, [(x + i\, y)/r_o]^n,$$

where l is the effective magnetic length for an integral measurement and B_o is the design main field. ($B' = B_o b_1/r_o$ and $B''/2 = B_o b_2/r_o^2$ are the gradient and second-derivative fields of quad and sext magnets, respectively.) The multipole coefficients are defined as $b_1 = 1.0$ and $a_1 = 0$ for a quad, and $b_2 = 1.0$ and $a_2 = 0$ for a sext magnet at a reference radius $r_o = 25$ mm.

Similar to the dipole data, the integrated quad fields at four excitation currents and the remanent fields are plotted in Figs. 5 and 6 for the SR 0.5-m quads. It has been identified that the steel laminations have three different

kinds of heat treatment, one for magnet numbers 1-200 and two for 201-250. The data replotted in Fig. 7 shows that those quads with Br'l higher than 0.064T have weaker B'l by 2 x 10^{-3} on average and the rms is relatively larger. It is also seen that the rms is larger at higher currents for all quads and the spread is even larger for those with higher Br'l. The asymmetrical shape of the histogram for the quad fields plotted in Fig. 8 is due to those different lamination properties.

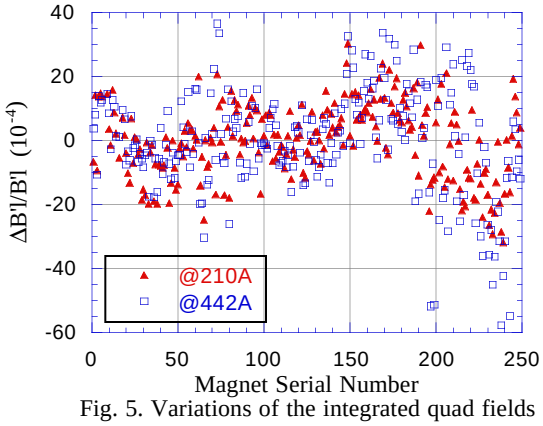

Fig. 5. Variations of the integrated quad fields for the SR 0.5-m quads.

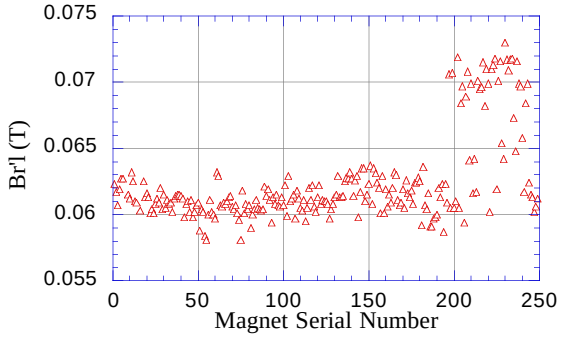

Fig. 6. Integrated remanent quad fields of the SR 0.5-m quads.

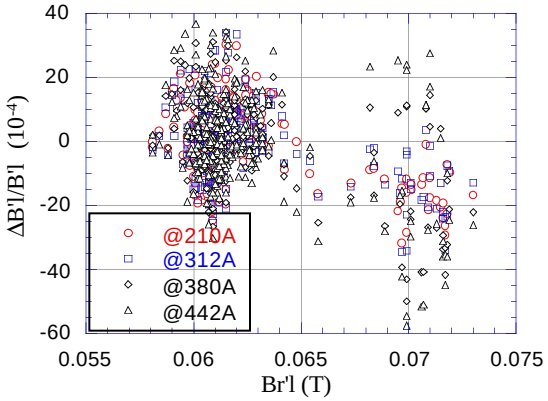

Fig. 7. Variationsof the integrated quad fields at four excitation currents vs. remanences for the 0.5-m quads.

A few "forbidden" multipole coefficients for the 0.5-m quads are plotted in Fig. 9. Even if the quads were assembled from four quadrants, Fig. 9 shows that both the normal and skew sext coefficients (b_2 and a_2) remain consistent on average during the assembly period. On the other hand, b_3 gradually increases by 2 x 10^{-4} over the period, which seems to be related to the increase of the B'l shown in Fig. 5 except for those quads with higher Br'l. This suggests a decrease in the gap between the top and bottom halves of the quads as the quad numbers increased. The data spread of the "allowed coefficient" b_5, shown in Fig. 10, is due to the dimensional tolerances of 20-mm-thick end-packs with end-bevels for the ends of the magnets. Other allowed higher coefficients hardly changed. During the whole period of the measurement, b_3 of the reference quad changed less than 0.2 x 10^{-4}.

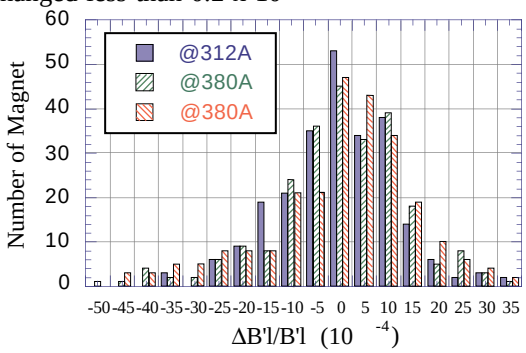

Fig. 8. Histogram of the integrated quad fields for the SR 0.5-m quads.

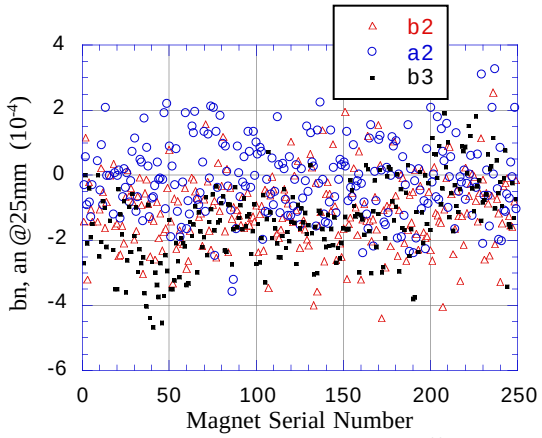

Fig. 9. "Forbidden" multipole coefficients for the SR 0.5-m quads.

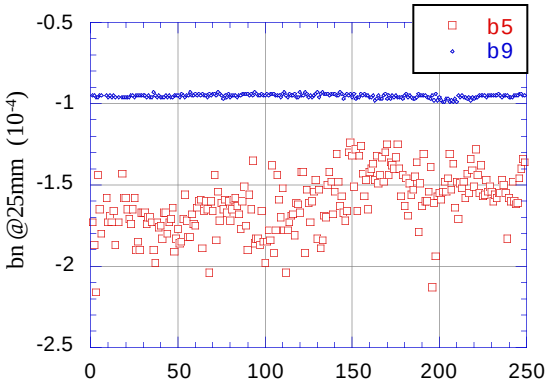

Fig. 10. "Allowed" multipole coefficients for the SR 0.5-m quads.

The axis of the rotating coil was aligned to the magnetic axis by adjusting the magnet position to where the dipole and quad field components of the quad and sext magnets, respectively, vanished. Prior to this procedure the

bore axis of the quad was aligned to the axis of the two air bearings defining the axis of the rotating coil using the following method. A laser beam unit was installed and aligned with the axis of the air bearing. A photo-quadrant detector was placed at the bore axis of the magnet aperture. After detecting the beam position along the bore axis, the magnet position was adjusted to align the bore axis to the laser beam. This procedure not only ensured parallelism between the bore and magnetic axes to at least ± 0.2 mrad, but it also enabled measurement of the offset of the two axes.

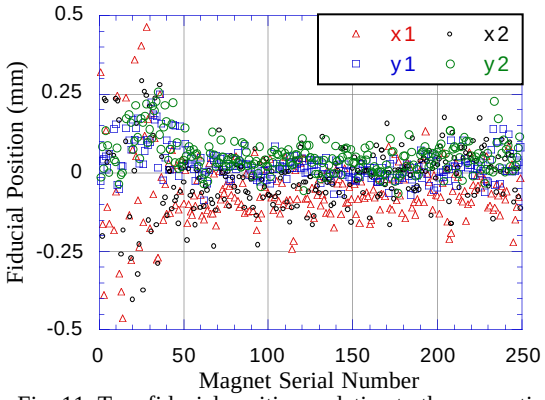

Fig. 11. Two fiducial positions relative to the magnetic axes. y1 and y2 have an offset of 384.629 mm.

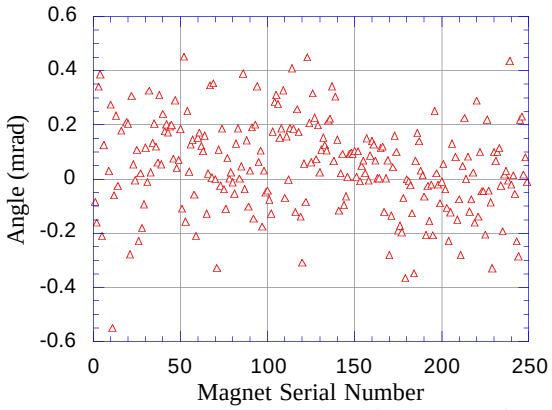

Fig. 12. The roll angles on top of the core surfaces when magnetically aligned for the 0.5-m quads.

Plotted in Fig. 11 are the two fiducial positions relative to the magnetic axis which were measured when the dipole components and the roll angles of the quad fields were zero. These fiducial ball bases were welded prior to the magnetic measurements. At the same time, the angle of the core surface on top of the magnet, shown in Fig. 12, was measured for the survey and alignment. The vertical positions have an offset of 384.629 mm. It is seen that the rms of the fiducal positions for the first 50 quads is relatively large, suggesting that it was a learning period of welding the fiducial bases to specified positions. It has been found that the horizontal positions and the angles have a relatively weak correlation; the average value of the horizontal positions, -0.058 mm, is due to a systematic error of the angle measurements by 0.15 mrad, assuming that dimemsional errors of the quads and the welded fiducial positions are random.

Shown in Fig. 13 is the offset of the magnetic and mechanical axes. During the magnetic alignment, a magnet was moved only in parallel from the mechanical axis. Therefore, only the average coordinate positions for the two fiducials are plotted. The average y-offset for all 0.5-m quads, -0.059 mm, is due to the fact that the diameter of a photo-quadrant detector used for the mechanical axis was 0.051 mm smaller than the quad aperture diameter.

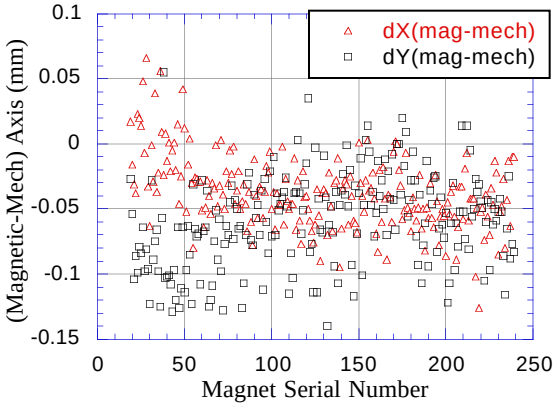

Fig. 13. The offsets between the magnetic and mechanical axes for the 0.5-m quads.

The measured data statistics for all 0.5-m, 0.6-m and 0.8-m quads are summarized in Table 2. The rms of the integrated field measurements of a 0.5-m reference quad for over a year was 1.1 x 10^{-4}, and those for the fiducial positions and the roll angle were 0.026 mm and 0.083 mrad, respectively.

Table 2
Measured data statistics for the SR quads.
ΔB'l/B'l in 10^{-4} unit, bn and an at r=25mm, and Δx and Δy are (magnetic-mechanical) axes.

	0.5-m Quad	.06-m Quad	0.8-m Quad
ΔB'l/B'l@312A	±11.17	±12.14	±6.92
ΔB'l/B'l@442A	±16.25	±10.79	±8.47
b2 (10^{-4})	-1.11±1.11	-1.0±0.86	-0.72±0.94
a2	-0.08±1.12	-0.01±01.03	0.15±0.85
b3	-1.42±1.22	-1.22±1.19	-0.86±1.10
b5	-1.61±0.18	-1.43±0.15	-1.24±0.15
b9	-0.95±0.012	-0.87±0.045	-0.75±0.010
Br'l (10^{-2} T)	6.24±0.33	7.36±0.15	10.28±0.16
θ (mrad)	0.046±0.177	0.096±0.175	0.108±0.221
Δx (mm)	-0.037±0.028	-0.034±0.032	-0.044±0.033
Δy (mm)	-0.059±0.036	-0.062±0.031	-0.048±0.031

C. Sextupole Magnet Data

The integrated sext fields and those of the remanence are plotted in Figs. 14 and 15 for the 280 sexts. It is seen that there are at least three levels of remanences. The data is replotted in Fig. 16 to see the correlation between the sext strength and the remanence. For sexts with lower Br"l than the average by 22%, the sext strengths are higher by 7 x 10^{-3} on average. It is seen also that the data spread is larger at higher current for all magnets and more severe for those with higher Br"l. The dipole field components at 150A and 0A are plotted in Fig. 17. The total dipole field

for all the sexts at 150A is approximately 3 x 10^{-4} of the 80 dipole magnets. The multipole coefficients and alignment parameters for the sexts are much less stringent compared to those for the quads.

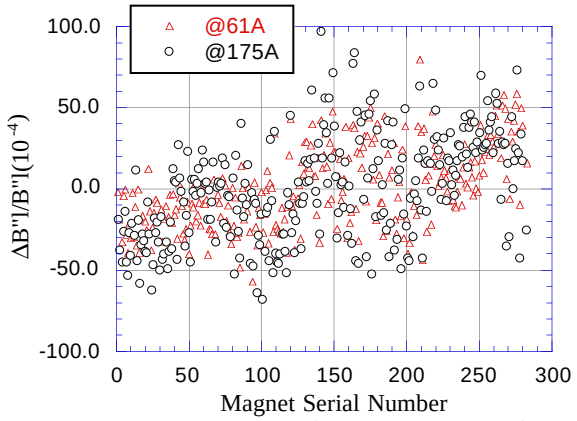

Fig. 14. Variations of the integrated sext fields for the SR sext magnets.

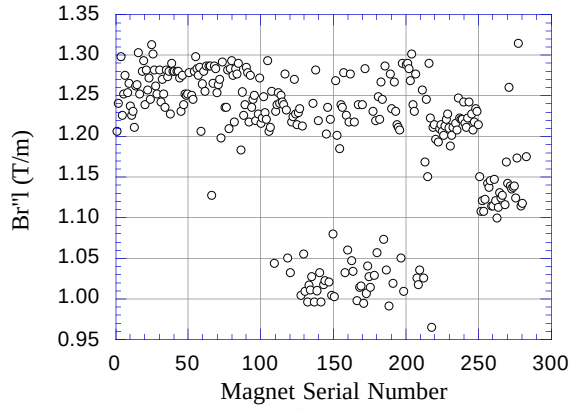

Fig. 15. Variations of the integrated remanent sext fields for the SR sexts.

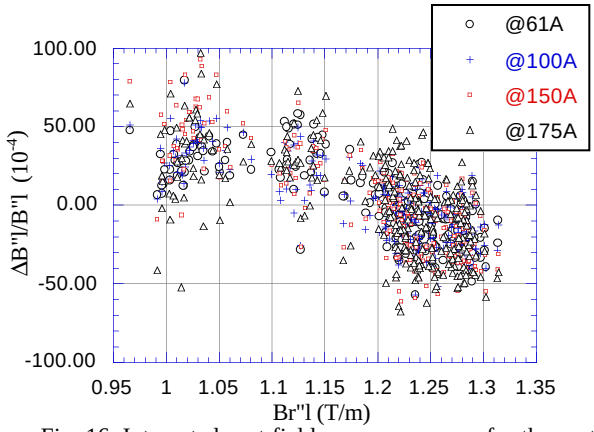

Fig. 16. Integrated sext fields vs. remanences for the sexts.

IV. SUMMARY

Measured data and allowed tolerances for the SR magnets are summarized in Table 3. For the dipoles, the use of laminations with different properties was a major factor for the data spread of dBl/Bl. Within ±25 mm of the transverse positions, the variation of dBl/Bl was less than 1 x 10^{-4}. Similarly, the data spreads of the field strengths for the quads and sexts were due to different lamination properties. Because of the use of individual power supplies for these magnets, the magnitude of the spread is not an issue. The consistency of the data for the multipole coefficents, the fiducial positions, the offsets of the magnetic and mechanical axes, and the roll angles indicate that the mechanical tolerances of the quad and sext magnets were well maintained during the entire magnet fabrication period. The rms of the fiducial position and roll angle for the reference 0.5-m quad data during the period of the production measurements were 0.025 mm and 0.12 mrad, respectively.

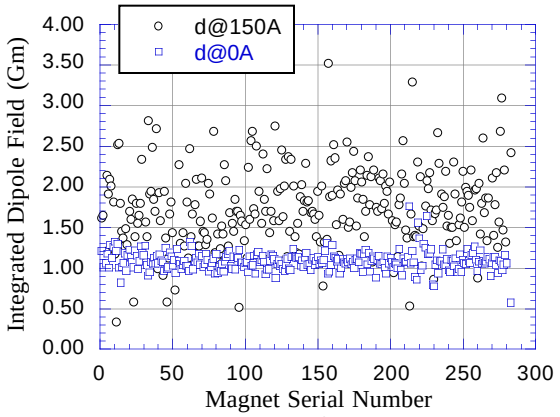

Fig. 17. Integrated dipole field components at 150A and remanences for the SR sexts.

Table 3
Data summary for the SR magnets. Relative field strengths and multipole coefficients are in 10^{-4}.

		measured average	measured rms	allowed tolerance
Dipoles	ΔBl/Bl		4.37	5.0
	b_1	-0.67	0.35	2.5
	b_2	0.94	0.10	3.1
Quads	ΔB'l/B'l		11.3	5.0
	b_2	-0.95	1.01	2.5
	a_2	-0.02	1.08	2.5
	b_3	-1.22	1.27	3.1
Sexts	ΔB"l/B"l		31.6	25.0
	b_3	0.76	2.45	31.0
	a_3	1.78	3.30	31.0
Reference	x,y (mm)		0.026	0.060
Quad	θ (mrad)		0.12	0.30

Measurment repeatabilites for dipole, quad, and sext were 1.5, 1.1, and 5 in 10^{-4} unit.

V. REFERENCES

[1] "7-Gev Advanced Photon Source Conceptual Design Report," Argonne National Laboratory, ANL-87-15, 1987, and J. N. Galayda, "The Advanced Photon Source," these proceedings.

[2] S. H. Kim, C. Doose, K. Kim and K. M. Thompson and L. R. Turner, "Performance of Quadrupole and Sextupole Magnets for the Advanced Photon Source," *IEEE Trans. on Magnetics*, Vol. 30, pp. 2612-2615, 1994.

[3] S. H. Kim, C. Doose, R. Hogrefe, K. Kim and R. Merl, "The Magnet Measurement Facility for the Advanced Photon Source," *IEEE Trans. on Magnetics*, Vol. 30, pp. 2616-2619, 1994.